Impact of Reduced Fluvial Sediment Supply on Saltwater Intrusion in the Yangtze Estuary

Zhu, Chunyan; van Maren, D. S.; Guo, Leicheng; He, Qing; Wang, Zheng B.

DOI
10.1029/2022EF003274

Publication date
2023

Document Version
Final published version

Published in
Earth's Future

Citation (APA)
Zhu, C., van Maren, D. S., Guo, L., He, Q., & Wang, Z. B. (2023). Impact of Reduced Fluvial Sediment Supply on Saltwater Intrusion in the Yangtze Estuary. *Earth's Future*, *11*(10), Article e2022EF003274. https://doi.org/10.1029/2022EF003274

Earth's Future

RESEARCH ARTICLE
10.1029/2022EF003274

Impact of Reduced Fluvial Sediment Supply on Saltwater Intrusion in the Yangtze Estuary

Chunyan Zhu[1,2], D. S. van Maren[1,2,3], Leicheng Guo[1], Qing He[1], and Zheng B. Wang[2,3]

[1]State Key Lab of Estuarine and Coastal Research, East China Normal University, Shanghai, China, [2]Faculty of Civil Engineering and Geosciences, Delft University of Technology, Delft, The Netherlands, [3]Deltares, Delft, The Netherlands

Key Points:

- A decline in riverine sediment supply weakens sediment–fluid interactions, thereby decreasing saltwater intrusion
- Saltwater intrusion may be as much influenced by a sediment load reduction as by changes in river discharge distribution or sea-level rise
- Predicting saltwater intrusion in highly turbid estuaries requires evaluation of the role of sediments before applying a noncoupled model

Supporting Information:

Supporting Information may be found in the online version of this article.

Correspondence to:

Q. He,
qinghe@sklec.ecnu.edu.cn

Citation:

Zhu, C., van Maren, D. S., Guo, L., He, Q., & Wang, Z. B. (2023). Impact of reduced fluvial sediment supply on saltwater intrusion in the Yangtze Estuary. *Earth's Future*, *11*, e2022EF003274. https://doi.org/10.1029/2022EF003274

Received 14 OCT 2022
Accepted 29 AUG 2023

Abstract A decline of the fluvial sediment supply leads to coastal erosion and land loss. However, the fluvial sediment load may influence not only coastal morphodynamics but also estuarine hydrodynamics and associated saltwater intrusion. Previous studies revealed that suspended sediments influence estuarine hydrodynamics through various flow–sediment interactions. In this contribution, we systematically investigate how changes in fluvial sediment load and other climate-change-induced environmental change influence estuarine hydrodynamics and sediment dynamics. For this purpose, we utilize a well-calibrated fully coupled model in which hydrodynamics, saltwater intrusion, and sediment transport interact with each other, to explore saltwater intrusion in the Yangtze Estuary in response to a decline in the sediment load, modified discharge, and sea-level rise. Model results suggest that a 70% decline in the suspended sediment load weakens the impact of sediments on salinity-induced stratification and thereby reducing saltwater intrusion. Sea-level rise or discharge peak reduction increases saltwater intrusion. However, a fully coupled model accounting for sediment effects predicts a much larger increase in saltwater intrusion compared to noncoupled models. Whether this effect is important depends on estuarine sediment concentrations and therefore the potential role of sediments should be carefully investigated before applying a noncoupled model. This work highlights not only the relevance of a suspended sediment decline but also the use of fully coupled models for predicting saltwater intrusion in turbid estuaries and has broad implications for freshwater resource management in turbid estuarine systems influenced by human interventions and climate change.

Plain Language Summary Saltwater intrusion is strongly influenced by river flow, tides, and morphology in estuaries. In highly turbid estuaries, high suspended sediment concentrations interact with salinity, which also plays an important role in saltwater intrusion and freshwater resources. However, many of these estuaries are suffering from a reduction in sediment supply, leading to reduced sediment concentration in recent decades. In this study, we employ a fully coupled three-dimensional numerical model to investigate the effect of reduced sediment supply on saltwater intrusion. The fully coupled model predicts a much larger increase in saltwater intrusion in response to sea-level rise or modulation of the river discharge compared to noncoupled models. In contrast, a decline in riverine sediment supply weakens sediment–turbulence interaction, thereby decreasing saltwater intrusion. These findings are important for the management of sediment and freshwater resources in turbid estuaries.

1. Introduction

Saltwater intrusion is the landward movement of saltwater under the combined influence of tidal forcing and river flow, which is also strongly influenced by channel geometry. The degree of saltwater intrusion influences not only directly estuarine ecology (Watanabe et al., 2014) and freshwater supply to densely populated deltas but also indirectly through its impact on sediment dynamics (van Maanen & Sottolichio, 2018; Wan & Zhao, 2017; Wolanski et al., 1996). Sediment dynamics additionally influence the ecological state of the estuary through its impact on the light climate (Talke et al., 2009), and drive siltation in tidal channels, often resulting in dredging requirements in urbanized delta systems (Hossain et al., 2004; Jeuken & Wang, 2010; van Maren, van Kessel, et al., 2015; S. Wu et al., 2016).

Saltwater intrusion is mainly controlled by river discharge, tide, wind, sea-level rise (SLR), and morphological changes. A high river discharge results in a reduced saltwater intrusion. The relationship between saltwater intrusion length and river discharge follows a power law with an exponent coefficient varying in different estuaries (Banas et al., 2004; Monismith et al., 2002). The effect of tides on saltwater intrusion is also closely

related to the degree of tidal mixing. For a well-mixed or salt wedge estuary, salt intrudes more landward during spring tides than during neap tides (Brockway et al., 2006; Ralston et al., 2010; Uncles & Stephens, 1996; Xue et al., 2009), whereas in partially mixed estuaries, the upstream salt flux is largest during neap tides (Banas et al., 2004; Lerczak et al., 2009; Monismith et al., 2002; Ralston et al., 2008). SLR increases water depth and benefits inland tidal propagation, which may strengthen estuarine circulation (Chua & Xu, 2014) and enhance saltwater intrusion (Prandle & Lane, 2015; Rice et al., 2012; Robins et al., 2016). Persistent northerly wind may enhance saltwater intrusion in the Yangtze Estuary by landward Ekman currents (L. Li, Zhu, et al., 2020; H. Wu et al., 2010; Xue et al., 2009). Strong wind events may also induce water level setup, an increase in flood current velocity, and a decrease in ebb-directed current velocity and freshwater inflow, enhancing saltwater intrusion (E. Zhang et al., 2019). Moreover, various human interventions have influenced the degree of saltwater intrusion, especially morphological changes resulting from channel deepening (S. Wu et al., 2016) or modifications in river discharge (Gong & Shen, 2011) or sediment transport (Eslami et al., 2019). In the future, such anthropogenic influences will only become more pronounced as a result of climatic change-induced shifts in precipitation patterns and SLR (Chen et al., 2016; Rice et al., 2012; Talke & Jay, 2020; van Maanen & Sottolichio, 2018), river discharge changes (Alfieri et al., 2015; Robins et al., 2016; Talke & Jay, 2020), and tidal channel deepening (van Maren, Winterwerp, et al., 2015; S. Wu et al., 2016).

Sediment dynamics are controlled by hydrodynamics, and at the same time, sediment dynamics may exert feedback to the hydrodynamics, thus affecting saltwater intrusion, particularly in highly turbid estuaries. High sediment concentrations suppress turbulence mixing, influence hydraulic drag, and thus affect tidal propagation. Many estuaries have regions of elevated suspended sediment concentrations (SSCs; i.e., estuarine turbidity maximum or ETM) resulting from converging sediment transport (Dyer, 1997). The residual sediment transport is strongly influenced by the salinity-induced density gradient (Festa & Hansen, 1978) and tidally varying stratification (Simpson et al., 1990). Therefore, ETMs are often located at the landward limit of saltwater intrusion. In turn, sediments also influence saltwater intrusion due to feedback between SSC, velocity, water level, salinity, and tidal amplification (C. Zhu, van Maren, et al., 2021) with higher SSC leading to stronger saltwater intrusion. Many river systems have experienced a decline in their sediment load resulting from the construction of upstream reservoirs (Besset et al., 2019; Dunn et al., 2019; L. Li, Ni, et al., 2020; J. P. Syvitski et al., 2009), which probably causes a reduction in sediment concentration in estuaries and then influences saltwater intrusion. However, the role of sediment dynamics on saltwater intrusion has so far remained unexplored.

The Yangtze Estuary is a strongly engineered system with regulated river flow, sediment load, and local geometry. Saltwater intrusion in the Yangtze Estuary has been studied both analytically (Cai et al., 2015; E. Zhang et al., 2011, 2019) and numerically (Chen et al., 2016; H. Wu et al., 2010; Xue et al., 2009; J. Zhu et al., 2018). Moreover, saltwater intrusion in the Yangtze Estuary has been studied for natural effects and climate change, that is, the effect of wind (L. Li, Zhu, et al., 2020; H. Wu et al., 2010; Xue et al., 2009; E. Zhang et al., 2019; J. Zhu et al., 2018) and SLR (Chen et al., 2016) as well as human interventions, for example, Three Gorges Dam (TGD), Deep Channel Navigation Project (DCNP), and Water Diversion Project (WDP), see J. Zhu et al. (2018). However, the impact of sediment dynamics on saltwater intrusion has not yet been investigated. This study numerically explores the effect of the changes in river discharge and sediment supply as well as SLR on altering the sediment dynamics and saltwater intrusion in the Yangtze Estuary.

2. Study Area

The Yangtze Estuary is a 650 km long estuary conveying large river discharge and sediment load supplied by the Yangtze River. The river discharge and sediment transport of the Yangtze River is highly variable, with river discharge ranging from 8,300 to over 90,000 m^3/s and SSC ranging from 0.01 to >3 kg/m^3. In the Yangtze River basin, two large projects regulate the river discharge and sediment load into the estuary: the TGD and WDP (Figure 1a). The TGD was constructed between 1993 and 2009 and put into operation in 2003 to store and flush water seasonally (L. Guo et al., 2018). Apart from the TGD, thousands of hydropower dams were built in the Yangtze River basin, altering the river flow seasonally and decreasing sediment supply to the estuary. Specifically, the high river discharge in the wet season decreases profoundly by ∼30% while the low river discharge in the dry season slightly increases by ∼10% due to the regulation, and the sediment load is reduced by 70% (L. Guo et al., 2018). The ongoing South-to-North WDP is a strategic project to mitigate water shortage in northern China. It includes three water transfer plans: the western, middle, and eastern route project. Since 2014,

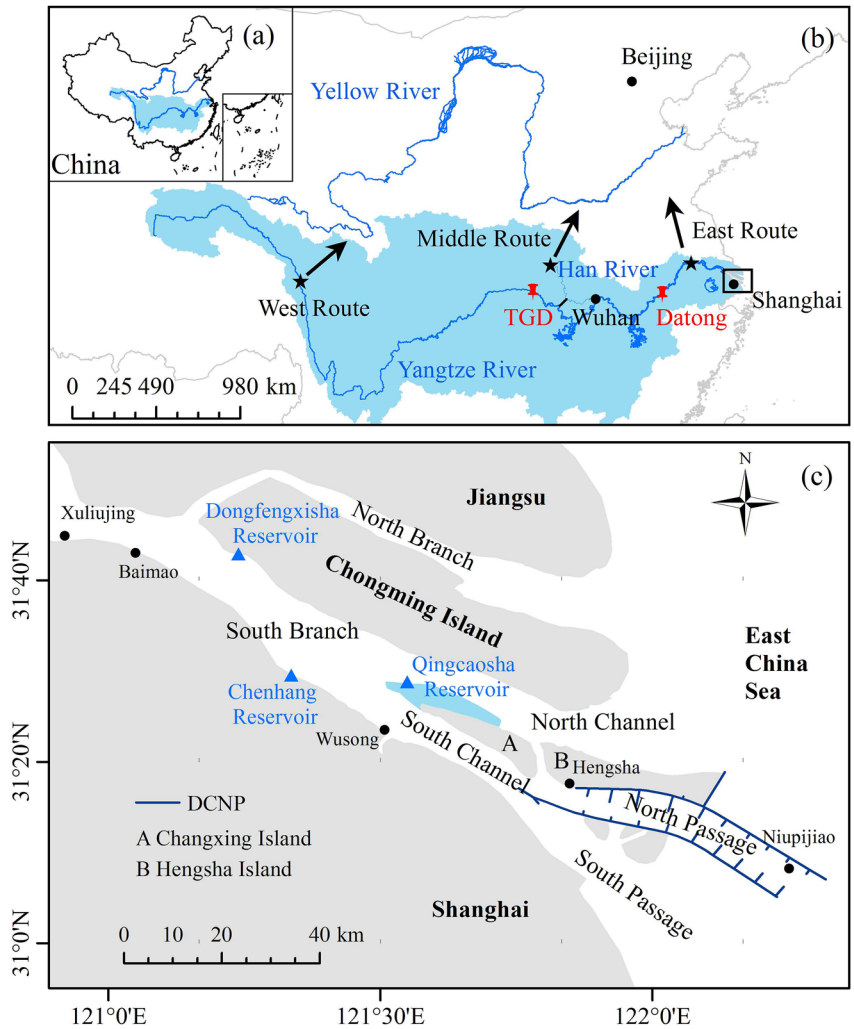

Figure 1. Map of (a) China, (b) South to North Water Diversion Project (WDP) and the Three Gorges Dam (TGD) in the Yangtze River basin (shade in blue), and (c) location of the freshwater reservoirs and saltwater intrusion paths in the Yangtze Estuary. DCNP, Deep Channel Navigation Project.

the WDP annually withdraws 18.3 billion m^3 of water from the Yangtze River basin, but when completed the total diversion capacity will be 44.8 billion m^3 per year (approximately 5% of the mean Yangtze River runoff; L. Guo et al., 2018). Moreover, extremely high floods occurred in 1954 (92,600 m^3/s), 1998 (82,300 m^3/s), and 2020 (84,500 m^3/s), over ~30% higher than the peak high river discharge in normal years. Relatively low river discharges are approximately 6,500–10,000 m^3/s, for example, in 1972 (7,060 m^3/s), 1979 (6,470 m^3/s), and 2006 (9,660 m^3/s), 10%–40% lower than the low river discharge in normal years.

The Yangtze Estuary is morphologically characterized by 3 orders of bifurcation and four outlets into the sea. Approximately 5% of the river discharge is flushed through the North Branch and the major portion of river flow is discharged in the South Branch and the seaward channels (Figure 1b). The Yangtze River supplies freshwater to Shanghai through three reservoirs, that is, Dongfengxisha Reservoir, Chenhang Reservoir, and Qingcaosha Reservoir. The Qingcaosha Reservoir was built in 2010 along northwestern Changxing Island (Figure 1c), which is the largest one supplying more than 70% of the freshwater for the 13 million people in Shanghai. The salinity in the Yangtze Estuary near the intake of Qingcaosha Reservoir is therefore crucial for freshwater availability and used in this study as a metric to evaluate the impact of sediment dynamics on saltwater intrusion. Saltwater intrusion in the North Channel can affect water intake of the Qingcaosha Reservoir from the seaside, while salt spillover in the North Branch adds additional influence from the land side (Chen et al., 2016; J. Zhu et al., 2018). Hence, it is of particular importance to understand the salt dynamics in the Yangtze Estuary.

3. Methods

3.1. Model Description

Past studies of saltwater intrusion were mainly based on analytical and numerical models. Analytical models have been used to predict saltwater intrusion length and longitudinal salinity distribution in estuaries. These analytical models can be used for simplified estuaries with prismatic and convergent channels (Prandle, 2004; Savenije, 2006) and can also account for tidal mixing under the river and tide forcing (Cai et al., 2015; Nguyen et al., 2012). More in-depth understanding of the mechanisms underlying saltwater intrusion in actual estuaries is obtained from three-dimensional (3D) numerical models (Cheng et al., 2012; Eslami, Hoekstra, Kernkamp, et al., 2021; Gong & Shen, 2011; Jeong et al., 2010; Ralston et al., 2010; J. Wang et al., 2019). In this study, we use a well-calibrated fully coupled 3D numerical model developed by C. Zhu, van Maren, et al. (2021). The full coupling herein refers to both salinity and sediment contributing to the fluid density, both thereby potentially damping turbulence and the driving gravity currents. Through complex feedback mechanisms, the SSC then influences water level, velocity, salinity, and in turn sediment. Note that including salinity-induced density effects is standard practice in numerical models, but including sediment-induced density effects (SedDEs) is not.

The 3D sediment transport model is set up using Delft3D (Lesser et al., 2004). The model application consists of hydrodynamic and sediment transport modules (C. Zhu, van Maren, et al., 2021). The hydrodynamics are computed for one full year (2007) with a realistic river discharge hydrograph and tidal forcing to capture the convergence of sediment. The sediment transport module is supply limited, with an ETM arising from sediment supplied from the model boundaries rather than initial bed conditions (see Brouwer et al., 2018; Dijkstra et al., 2018; Hesse et al., 2019; van Maren et al., 2011, 2020; C. Zhu, van Maren, et al., 2021). This approach allows the establishment of equilibrium sediment response to subtle variations in hydrodynamic conditions (in contrasts with an alluvial bed approach, where the amount and location of bed sediment dominate ETM dynamics and location). Although the model keeps track of erosion and deposition rates through sediment availability, it does not account for morphologic updates. The sediment concentration contributes to the water density through the equation of state, thereby generating the SedDEs introduced above. The main SedDE results from horizontal density gradients (leading to a gravitational circulation comparable to that of salt) and suppression of turbulence mixing by vertical concentration gradients (see C. Zhu, van Maren, et al., 2021 for details). The SedDE can be optionally switched off, as will be done to quantify the effect of sediments.

3.2. Model Performance

The Yangtze Estuary model is calibrated for the water level, velocity, salinity, and sediment concentration. Both simulated water level and velocity show good agreement with observations (see Supporting Information S1). The model captures the salinity distribution and its effect on the convergence of sediment, despite some discrepancies in the location and magnitude (Figure 2). The largest discrepancy is that the simulated near-bed SSC in the ETM is approximately 1.5 kg/m^3 which is smaller than observations. The low near-bed sediment concentration may result from multiple reasons which have been discussed in C. Zhu, van Maren, et al. (2021), such as exclusion of flocculation and consolidation processes, limited lateral water and sediment exchanges due to blocked jetties and groins, and the near-bed grid resolution. Our underestimations of the actual sediment concentrations would suggest that our model underestimates the impact of SSC on ETM dynamics and saltwater intrusion (which will be presented in the following section). At the same time, modeling the impact of sediments on hydrodynamics introduces a range of uncertainties (see e.g., van Maren et al., 2020; C. Zhu, van Maren, et al., 2021; C. Zhu et al., 2022). We believe that these uncertainties as well as the underestimation of SSC influence the magnitude of the response, but to a lesser degree the type of response. In our interpretation of model outcome, we therefore focus on the type of response (landward/seaward migration of ETM and salt wedge), rather than the distance they migrate. Given the complexities of modeling ETM dynamics in supply-limited conditions (as in our model) and with high near-bed SSC, we believe that our model sufficiently captures SSC, salinity, and the interaction between SSC and salinity and that its deviations from observations do not negate the main findings in this work.

3.3. Model Scenarios

We define a number of simplified discharge and sediment load scenarios in order to systematically evaluate the model response to such changes. These scenarios represent human interventions but may also be used to interpret

10.1029/2022EF003274

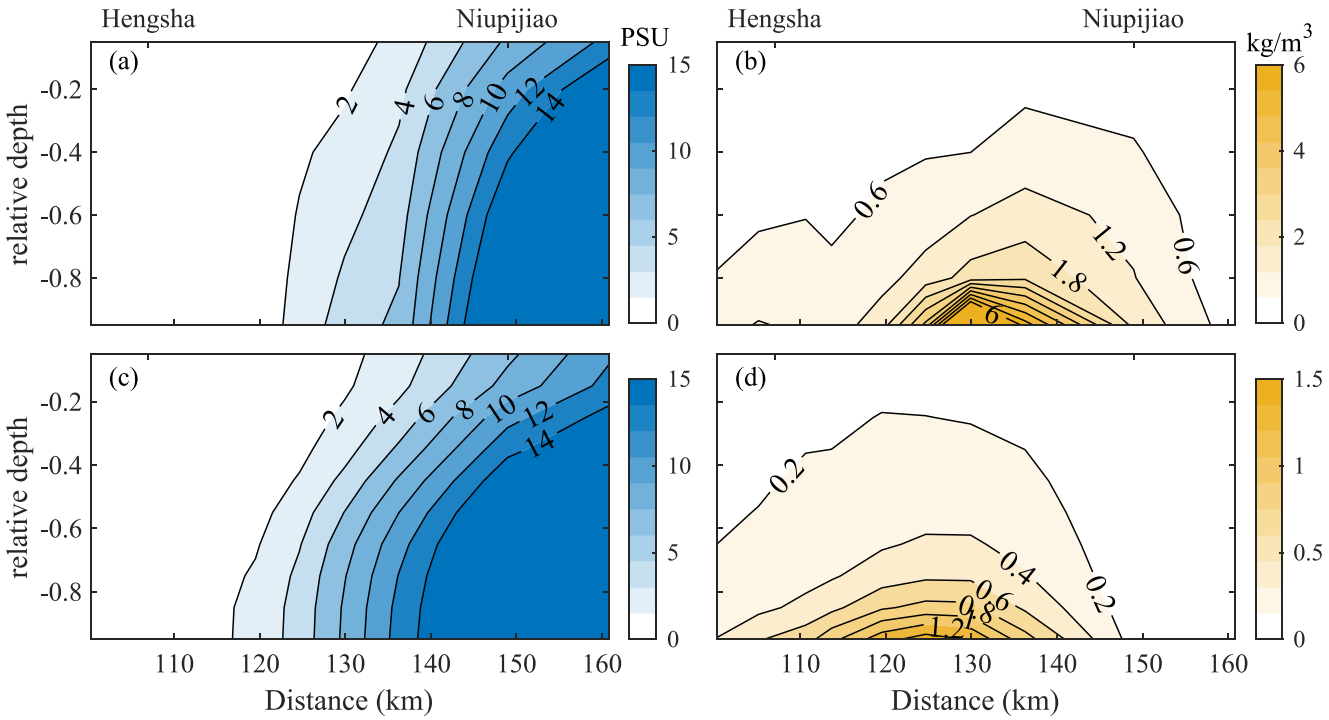

Figure 2. Observed (a, b) and modeled (c, d) distribution of tidally averaged salinity (a, c) and sediment concentration (b, d). The observed data are averaged over a tidal period from 14 to 15 August 2007 (see Supporting Information S1). The modeled salinity and SSC are averaged over the wet season (May–October).

climate change impacts, as will be elaborated in more detail in Section 5. To exclude the effect of variations in river discharge and sediment load from our model simulations, we impose simplified river discharge and sediment hydrographs, based on observations (Figure 3). We hereby assume that (a) there is only one significant flood peak each year and the hydrograph is symmetric; (b) there is no time lag between the river and sediment supply, and therefore the simplified hydrograph for sediments is also symmetric; (c) there is a linear relationship between the river discharge and SSC and therefore the seasonal variation of the SSC is the same as that of the river discharge. We construct two hydrographs with the same annual water discharge (878 billion m^3) but with a different seasonal variation, representing the pre-TGD ("HG-Q1") and post-TGD situations ("HG-Q2"). The post-TGD ("HG-Q2") accounts for the effect of dam constructions on reducing the seasonal variability of the river discharge compared to the pre-TGD ("HG-Q1"), that is, the maximum river discharge is reduced by 30%, and the minimum river discharge is increased by 10%. A third hydrograph ("HG-Q3") represents a 20% reduction in river discharge (relative to HG-Q1) reflecting current trends (a 50 billion m^3/year reduction over the period 1961–2019; Shi et al., 2022) and future water extraction (for expanding industry, agriculture, and urban use, but also the 45 million m^3 which will be diverted from the Yangtze to the drier North). The sediment load is computed using rating curves. Two types of sediment rating curves are used: one resulting in an annual sediment loads of 486 Mt $year^{-1}$ ("HG-S1," representing pre-TGD conditions) and 146 Mt $year^{-1}$ ("HG-S2," representing the observed 70% reduction in sediment load by the TGD). Finally, we evaluate the impact of SLR by running a scenario with 1-m higher sea level.

To explore the effect of changes in river discharge, SLR, and sediment supply on saltwater intrusion, the various boundary conditions are combined into a series of sensitivity scenarios (Table 1). The effect of SLR is evaluated by using an increase in the average water level of 1 m.

4. Results

4.1. Effect of Changes in Boundary Conditions

The changes in river flow, SLR, and sediment supply alter the sediment trapping and saltwater intrusion (Figure 4). For all scenarios, the highest near-bed SSC in an ETM occurs at approximately km-120 (between Hengsha and Niupijiao). Under equal annual streamflow and sediment load, the reduced seasonal variability in river discharge

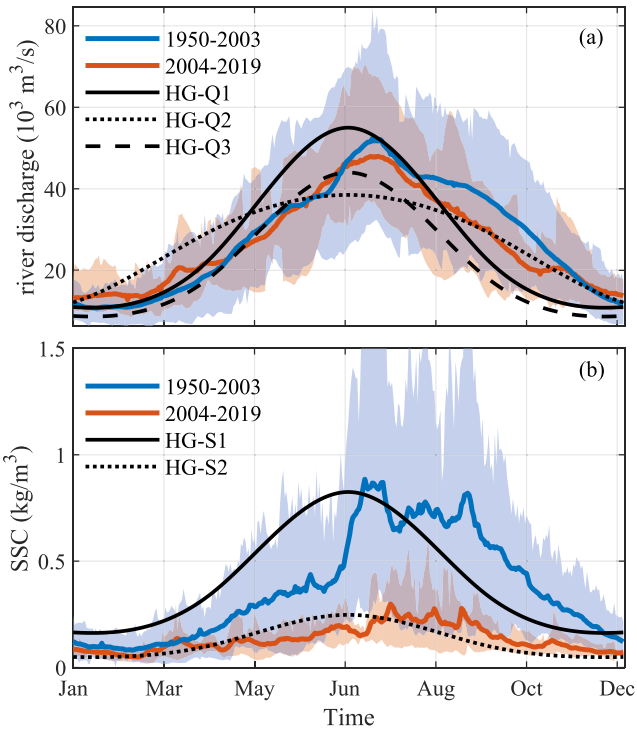

Figure 3. Simplified hydrographs of (a) river discharge (HG-Q1, HG-Q2, and HG-Q3) and (b) suspended sediment concentration (SSC; HG-S1, HG-S2) at Datong according to the measurement in the pre-Three Gorges Dam (pre-TGD; 1950–2003) and post-TGD (2004–2019) periods. The blue and red lines are the mean values of the pre- and post-TGD periods, whereas the shades indicate the variation range.

weakens saltwater intrusion (C1-sed). A 20% reduced annual river discharge leads to stronger saltwater intrusion (C2-sed). But among all evaluated scenarios, a SLR of 1 m (C3-sed) has the largest impact on saltwater intrusion with a landward migration of the 5 psu isohaline of approximately 10 km (compared to the reference C0-sed). On the other hand, saltwater intrusion is several km less for a scenario with a decline in sediment load (compare Figures 4e with 4a). Note that the effect of changes in boundary conditions on residual current can be found in Figure S8 in Supporting Information S1.

The various scenarios influence not only the annually averaged longitudinal distribution of SSC and salinity but also their seasonal variation (Figure 5). A flattened river discharge hydrograph moves the ETM (with a maximum SSC of ~20 kg/m^3) seaward in the dry season due to higher river discharges in that period. In contrast, the ETM moves landward and reaches a maximum SSC of >30 kg/m^3 when the annual streamflow reduces or the mean SLRs by 1 m compared with the reference scenario (Figure 5a). In the wet season, a decrease in river discharge and SLR enhance sediment trapping (compared to the reference scenario C0-sed). The strongest sediment trapping occurs for SLR of 1 m with the maximum SSC of >30 kg/m^3 (Figure 5b). In contrast, a 70% reduction in sediment supply results in SSC values in the ETM an order of magnitude lower. The maximum SSC of the ETM is slightly larger in the dry season (~2 kg/m^3) than the wet season (~1 kg/m^3).

Lower river discharges and SLR lead to stronger saltwater intrusion (Figures 5c and 5d). For instance, the C2-sed (11,148 m^3/s) and C1-sed (20,221 m^3/s) scenarios represent the lowest and highest mean river discharges in the dry season, and correspond to the weakest and strongest saltwater intrusion, respectively. However, 1 m of SLR (C3-sed) causes more saltwater intrusion than the modification of the river discharge (Figure 5c). The effect of the river discharge and SLR on saltwater intrusion is much less pronounced in the wet season (Figure 5c). The 70% reduction in sediment supply weakens saltwater intrusion in the dry and especially the wet season.

4.2. Effect of Coupling Sediments

To evaluate the effect of sediments, we compared the model results between the scenarios executed with a fully coupled model (including sediment–hydrodynamic interactions) and a noncoupled model, by examining

Table 1
List of Model Scenarios

Notes	Cases	River discharge hydrograph	SSC hydrograph	SLR (m)	SedDE
Reference	C0-sed	HG-Q1	HG-S1	0	Y
Changes in boundary conditions	C1-sed	HG-Q2	HG-S1	0	Y
	C2-sed	HG-Q3	HG-S1	0	Y
	C3-sed	HG-Q1	HG-S1	1	Y
	C4-sed	HG-Q1	HG-S2	0	Y
Without sediment effects	C0-hydro	HG-Q1	HG-S1	0	N
	C1-hydro	HG-Q2	HG-S1	0	N
	C2-hydro	HG-Q3	HG-S1	0	N
	C3-hydro	HG-Q1	HG-S1	1	N
	C4-hydro	HG-Q1	HG-S2	0	N

Note. Hydrographs for river discharge (HG-Q1, HG-Q2, and HG-Q3) and suspended sediment concentrations (SSCs; HG-S1 and HG-S2) refer to Figure 3. "HG-Q3" represents a 20% reduction in river discharge proportional to hydrograph "HG-Q1." SedDE, sediment-induced density effect. SLR, sea-level rise.

10.1029/2022EF003274

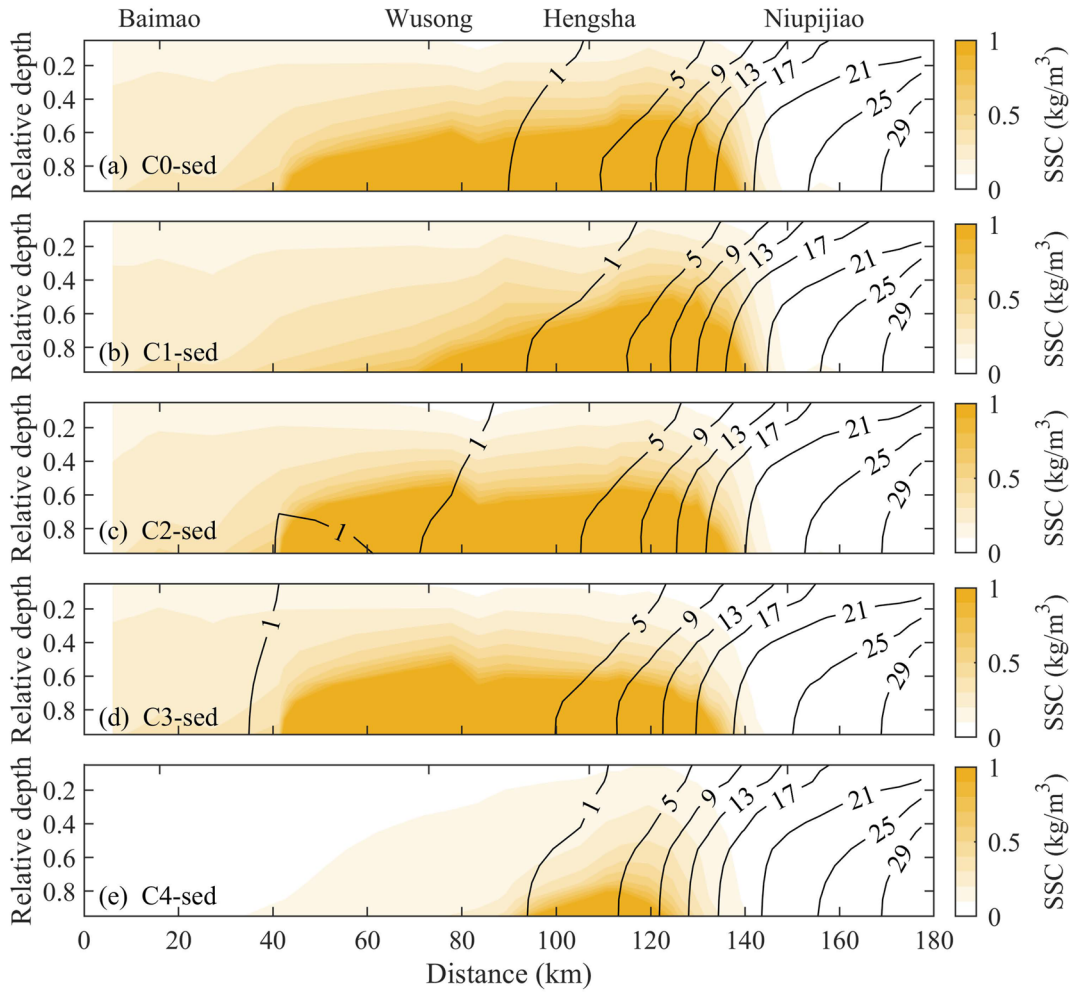

Figure 4. Modeled longitudinal distribution of salinity (black contour lines) and suspended sediment concentration (SSC; color shading) in scenarios (a) C0-sed, (b) C1-sed, (c) C2-sed, (d) C3-sed, and (e) C4-sed (see Table 1).

the differences in the surface and bottom salinity in the sensitivity scenarios compared to the reference case (Figures 5e–5h).

The effect of sediments on surface salinity indicates different spatial variations between the dry and wet season (Figures 5e and 5f). In the dry season, the fully coupled model predicts a higher surface salinity upstream of km-110 and downstream of km-160 (and a lower salinity in between) compared to the noncoupled model (Figure 5e). These changes in surface salinity are related to the variability in SSC. In the dry season, full coupling leads to a reduction in surface salinity in the part of the estuary where SSC is increasing in the landward direction (the seaward part of the ETM) and to an increase in surface salinity where SSC is decreasing in the landward direction (the most upstream section of the ETM). In the wet season, the increase in surface salinity occurred mainly offshore rather than the area with large horizontal SSC gradients and therefore the effects are relatively limited (Figure 5f).

Full coupling leads to an overall increase in the bottom salinity in both the dry and wet season (Figures 5g and 5h). In the dry season, the increase in bottom salinity is also closely related to the ETM location (Figure 5g). High SSC values (Figures 5a and 5b) lead to larger increase in bottom salinity; however, the more positively skewed shape of ETM corresponds to more uniform increase in salinity along the estuary. Specifically, the maximum increase in bottom salinity (>2 psu at km-110 in the scenario C3-sed) occurs for both high SSC and a positively skewed ETM shape. A 70% reduction in sediment supply leads to the weakest sediment convergence and therefore the smallest increase in bottom salinity, that is, the most pronounced increase occurs at km-110 by ~1 psu. In the wet season, the increase in bottom salinity is constrained downstream of km-90 (Figure 5f).

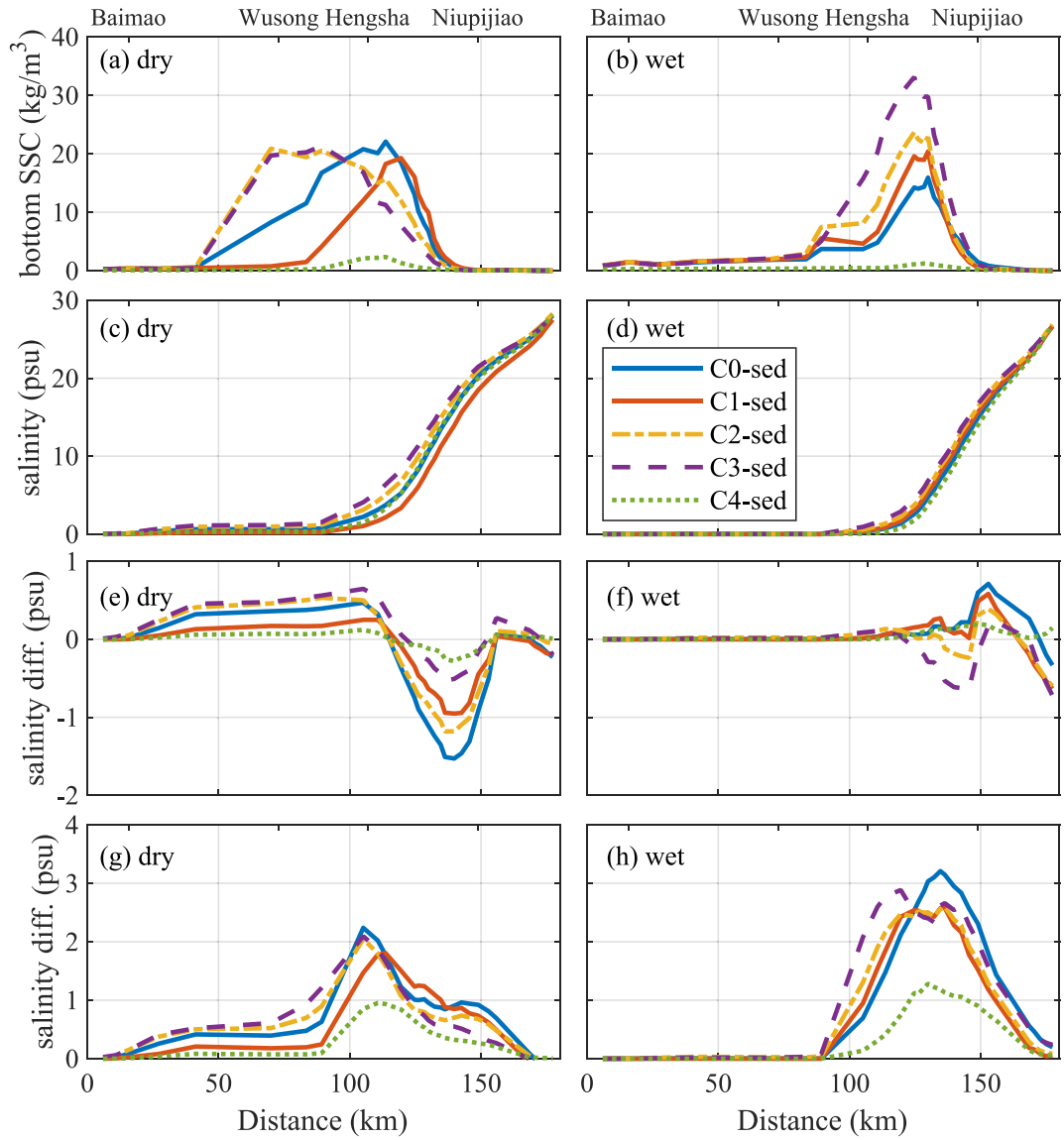

Figure 5. Modeled longitudinal variations of the bottom suspended sediment concentration (SSC; a, b), depth-averaged salinity in the fully coupled model (c, d), and salinity differences between the scenarios with a fully coupled and a noncoupled model in the surface (e, f) and bottom (g, h) layers in the dry (October–March, left) and wet (April–September, right) seasons (scenarios see Table 1). Positive value indicates an increase in salinity with the effects of sediment than without.

The different changes in the surface and bottom salinity induced by full coupling suggest changes in sediment-induced stratification, which is illustrated by longitudinal and vertical variability of the 0.75 psu isohaline (Figure 6). In the dry season, sediment-induced coupling causes pronounced landward shift of the median isohaline both near the surface and bottom than noncoupling with the "HG-Q1," "HG-Q3" hydrographs, and SLR (Figures 6a, 6e, and 6g). Specifically, the median isohaline near the surface shifts landward by 51, 27, and 33 km, respectively, with coupling than noncoupling. For flattening river discharge (C1) and reduced sediment load (C4), the landward migration of surface median isohaline is minor (by 1.9 and 2.3 km, respectively), whereas the median isohaline in the bottom moves landward by 20 and 11 km, respectively (Figures 6c and 6i). The landward movement of the bottom isohaline due to the sediment coupling is much smaller in C1 and C4 than for the other scenarios simply because ETM extension is limited and less sediment is available (see Figures 4 and 5a). In the wet season, sediment-induced coupling induces less than 1-km landward movement of the median isohaline near the surface for all scenarios compared to noncoupling (Figures 6b, 6d, 6f, 6h, and 6j). Near the bottom, sediment effects lead to the landward movement of the median isohaline by 11, 12, 13, 14, and 2 km,

10.1029/2022EF003274

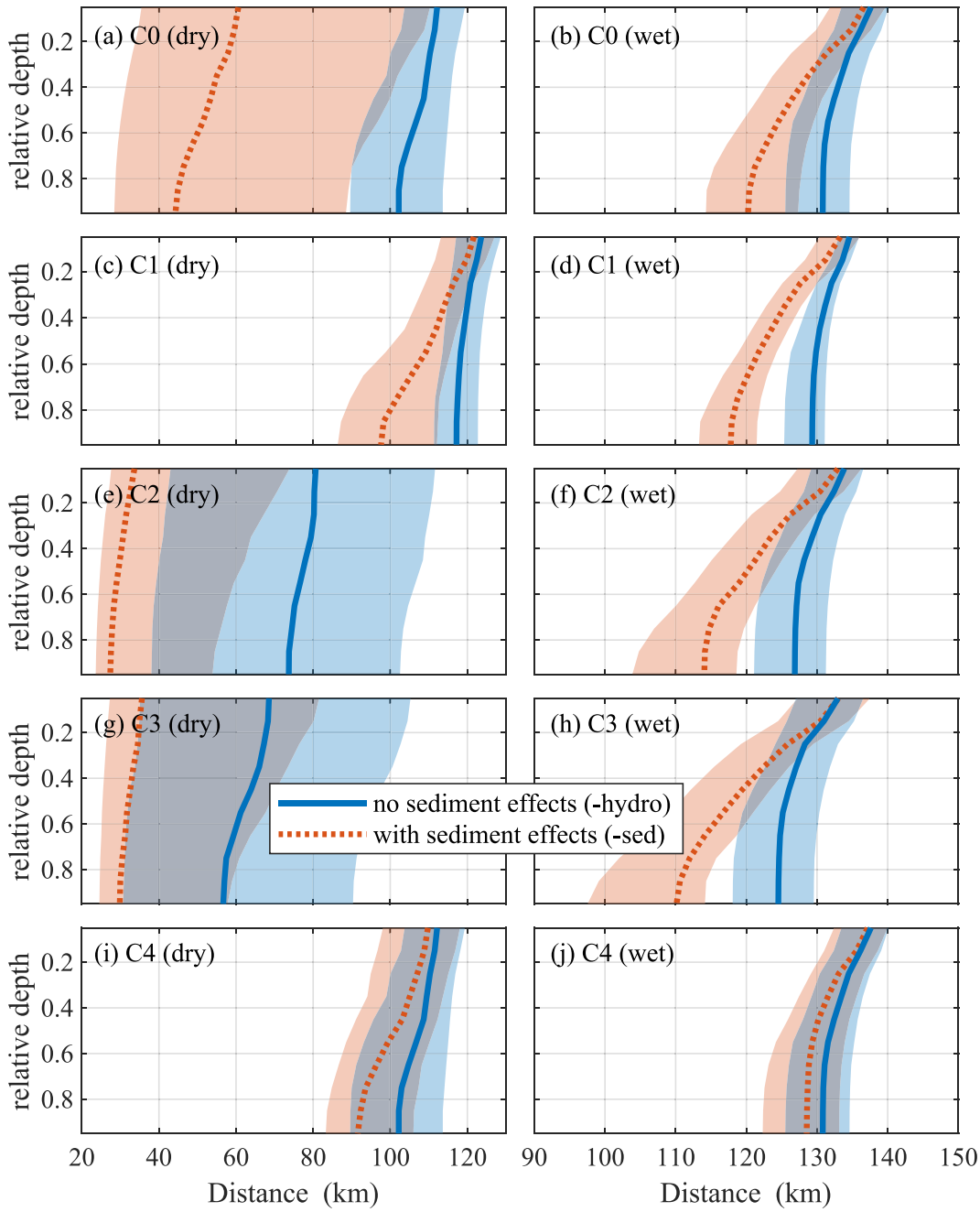

Figure 6. Comparison of the modeled vertical variation of the median location and variability of the salt front (defined as the intersection of the 0.75 psu isohaline from the surface to bottom) between the scenarios without effects of sediments (in blue, scenario names with "-hydro") and with the sediment effects (in red, scenario names with "-sed") in the dry (left) and wet season (right). Scenarios include (a, b) C0, (c, d) C1, (e, f) C2, (g, h) C3, and (i, j) C4 (see Table 1). The shades indicate the interquartile range of the location. The range in distance displayed here is different from the other figures to indicate the clear changes in stratification.

respectively. The difference of median isohaline near the surface and bottom suggests that salinity-induced stratification is enhanced by the effect of sediments particularly in the wet season.

The sediment load of the Yangtze Estuary is decreasing (Yang et al., 2014) and consequently this sensitivity of saltwater intrusion to sediment supply is important. We therefore evaluate the response of saltwater intrusion to sediment decline in more detail in the next section.

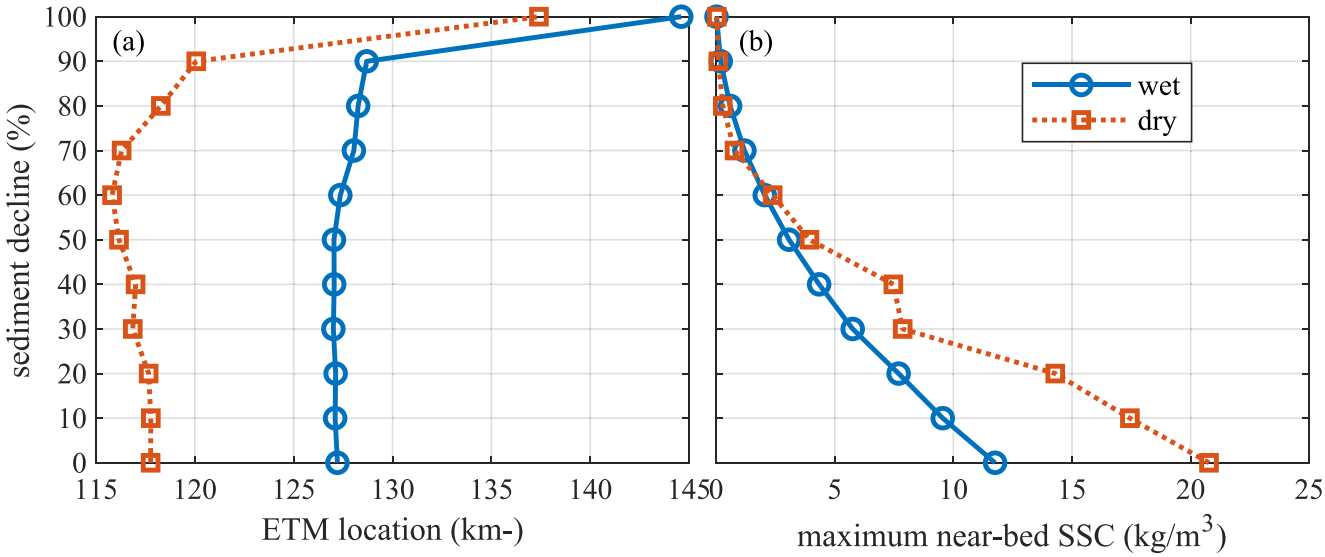

Figure 7. The changes in the location (a) and magnitude (b) of the maximum suspended sediment concentration (SSC) of the estuarine turbidity maximum (ETM) under stronger sediment decline from 0% to 100% for dry and wet season conditions with a river discharge of 20,000 and 40,000 m^3/s, respectively. All scenarios are computed with a fully coupled model.

4.3. Effect of Reduced Sediment Supply

To better understand the effect of the sediment supply, the model sensitivity to a sediment decline ranging from 0% to 100% is systematically evaluated with increments of 10% for dry season (constant river discharge of 20,000 m^3/s) and wet season (constant river discharge of 40,000 m^3/s) conditions, respectively. The initial SSC without sediment decline (sediment decline 0%) is constant for the wet season (0.36 kg/m^3) and dry season (0.27 kg/m^3) which are comparable to actual conditions in the Yangtze River. These scenarios are executed for 1 year and 4 months in which only the last 2 months are used for analysis, while the previous period allows the model to reach an equilibrium state.

The changes in the location and magnitude of the maximum SSC of the ETM quantitatively illustrate the important role of sediment decline (Figure 7). With stronger sediment decline, the ETM migrates landward with the maximum landward shift occurring at a sediment decline of 60% and 50% for a river discharge of 20,000 and 40,000 m^3/s, respectively. The maximum SSC of the ETM decreases with stronger sediment decline. This decrease is probably caused by weakening of the ETM, as suggested by the reduction in SSC in the ETM (Figure 7b). Interestingly, the sediment decline also influences the seasonal variation of the maximum SSC in the ETM. Specifically, the maximum SSC is larger in the dry season than in the wet season when the sediment decline is <60% (with a maximum SSC of 21 and 12 kg/m^3 at sediment decline by 0% for dry and wet season conditions, respectively).

The sediment decline also influences saltwater intrusion: see the computed changes in the median location of the surface and bottom salt front (Figure 8). The bottom salt front moves seaward with a reduction in SSC regardless of the riverine and tidal strength, varying from tens of meters to 20 km. The surface salt front may either move landward or seaward with stronger sediment decline. The landward migration of the surface salt front mainly occurs at neap tides, under relatively weaker (0%–50% reduction) and stronger (40%–100% reduction) sediment decline in the dry (Q = 20,000 m^3/s) and wet season conditions (Q = 40,000 m^3/s), respectively. At spring tides, the surface salt front may slightly move landward when sediment decline is less than 40% and mainly moves seaward when sediment decline is larger than 40%. Note that the bottom salinity moves further landward at neap tides than at spring tides, whereas surface salinity moves further landward at spring tides than at neap tides. This is caused by the stronger stratification at neap tides than spring tides as stronger tidal flow favors vertical mixing.

In the dry season, sediment coupling has the largest impact on the location of the salinity front during spring tides (especially near the surface), whereas its effect is largest during neap tides in the wet season (especially near the bed). This complex relationship is illustrated with timeseries of the salt front location in Figure 9. During

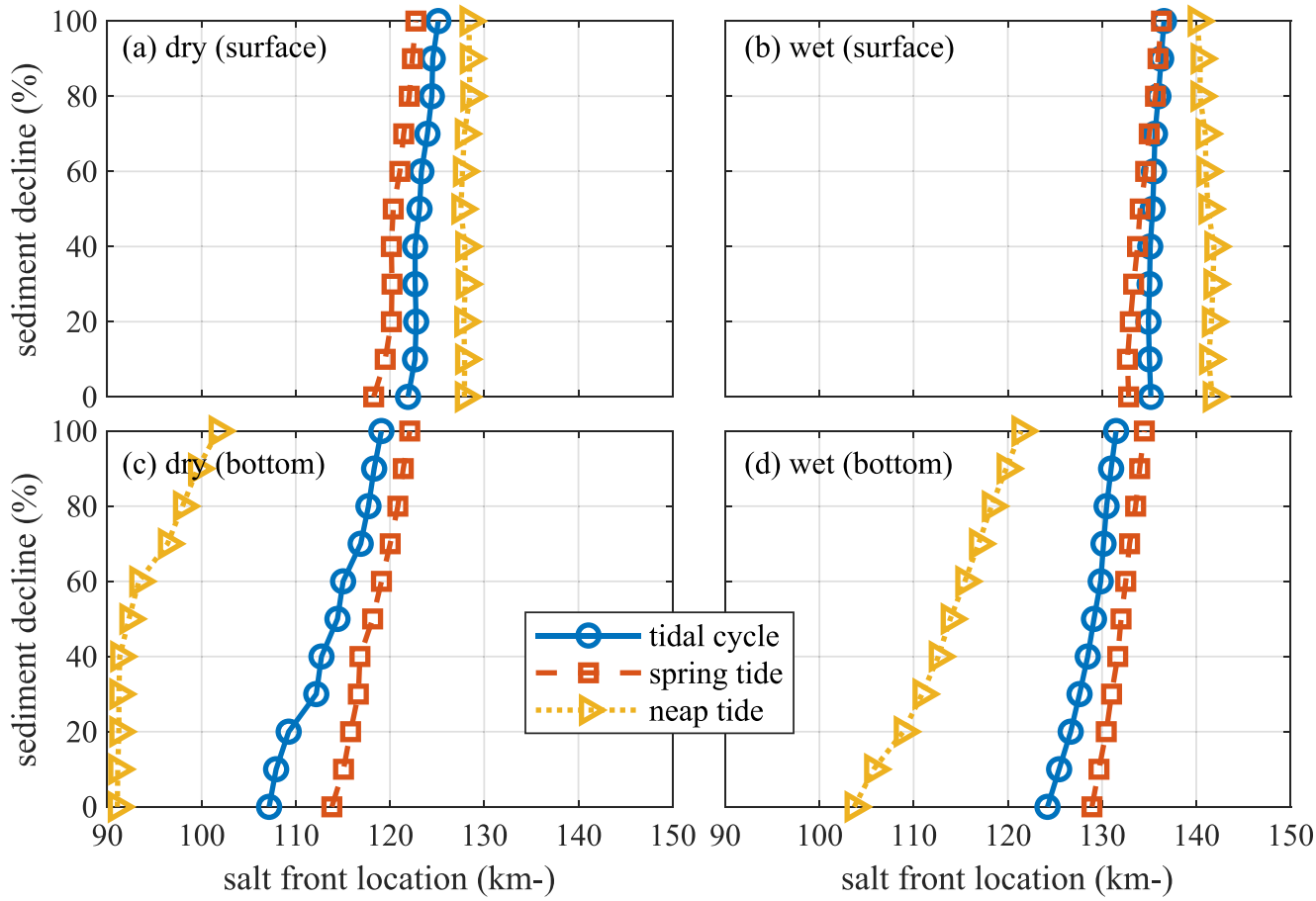

Figure 8. The median surface (a, b) and bottom (c, d) salt front location during spring tides (18–23 March), neap tides (11–16 March) tides and over the complete spring-neap tidal cycle (10–25 March) as a function of sediment decline (from 0% to 100%) in the dry season (a, c) and wet season (b, d); computed with a fully coupled model.

dry season conditions (Q = 20,000 m^3/s), the bottom salt front moves seaward as the sediment load declines. This effect is stronger at spring tides than at neap tides and maximum at intermediate tides. During wet season conditions (Q = 40,000 m^3/s), the seaward movement of the bottom salt front due to sediment decline is stronger at neap tides than at spring tides.

4.4. Impact on Freshwater Supply

The saltwater intrusion in winter (dry season) threatens the freshwater supply of the city of Shanghai. Typically, a salinity level of 0.25 psu is the limit for freshwater intake (M. Li & Chen, 2019). The number of days without freshwater is ~68 at Chenhang Reservoir in 2007 (Tang et al., 2011). The longest period without freshwater supply is ~54 consecutive days at Qingcaosha Reservoir in 2008 (J. Zhu et al., 2013). The reference scenario (C0-sed) of our numerical model simulated in 2007 reasonably reproduces the number of days without freshwater supply when defining a critical salinity limit of 0.75 psu (71 days without freshwater at Chenhang Reservoir and 54 consecutive days without freshwater at Qingcaosha Reservoir, see Table 2).

The modeled number of days without freshwater supply (using a surface salinity of >0.75 psu at Qingcaosha Reservoir) for various river discharge, SLR, and sediment supply scenarios is summarized in Table 3 (note that without full coupling, scenarios C0-hydro and C4-hydro are the same). For present-day conditions (including the effect of sediments; scenario C0-sed), the period without freshwater supply at km-75 is 102 days. These number of days decrease when the discharge is more evenly distributed over the year (C1-sed) but increase when the river discharge decreases (C2-sed) because of a discharge reduction in winter. SLR leads to 53 more days without freshwater availability (compared to the reference), suggesting a potential shortage in freshwater for the Shanghai

10.1029/2022EF003274

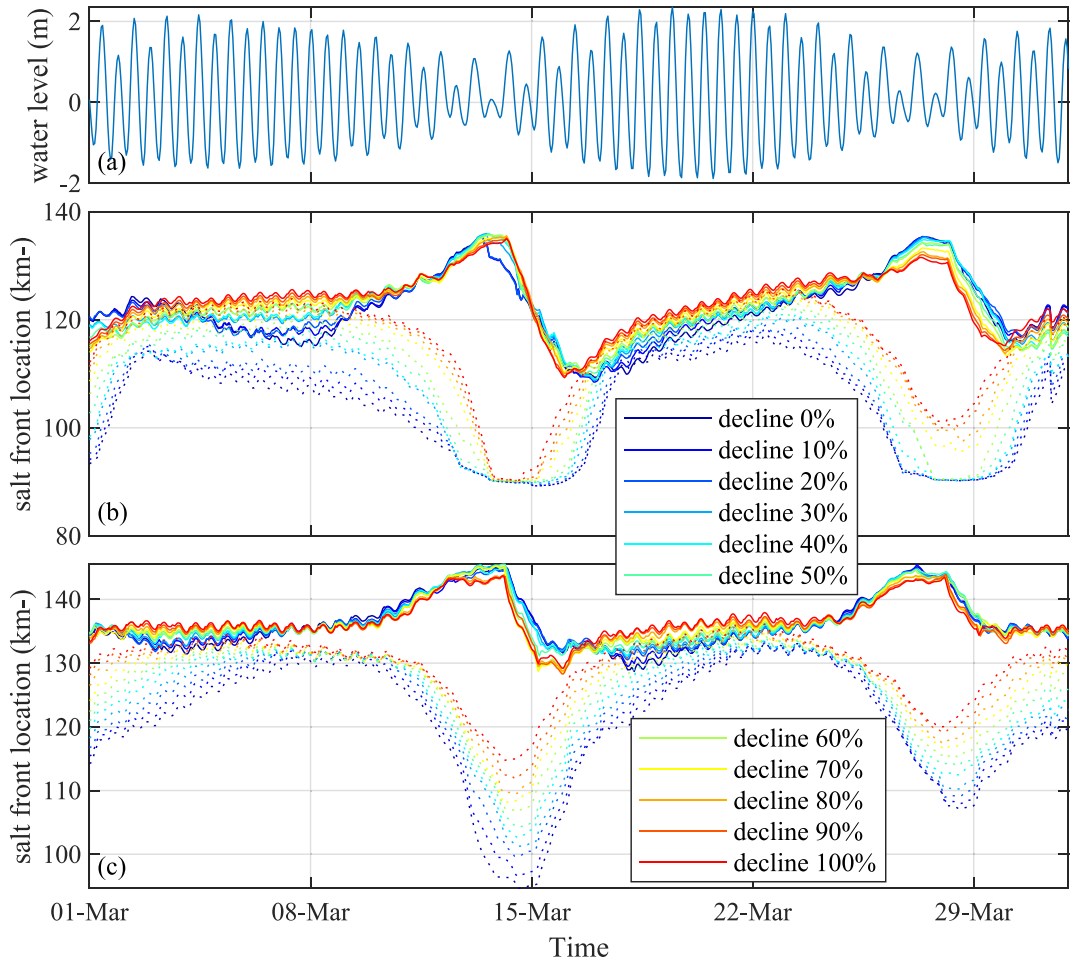

Figure 9. (a) Water level at Niupijiao in the wet season (see Figure 1) and the salt front locations of surface (solid lines) and bottom (dotted lines) salinity of 0.75 psu in response to sediment decline from 0% to 100% for (b) dry season and (c) wet season discharge conditions.

area. However, reducing the sediment load with 70% (C4-sed) leads to a 76% reduction in number of days with insufficient freshwater supply, potentially alleviating the freshwater intake problem near Shanghai. Therefore, the effect of sediments on the freshwater intake is explored in more detail by comparing scenarios with and without the effect of sediments.

Without a fully coupled model, the reference conditions (C0-hydro) reduce the number of days without freshwater from 102 to 21. A SLR of 1 m (scenario C3-hydro) yields the largest number of regular days without freshwater

Table 2
Modeled and Observed Number of Regular Days and Consecutive Days of the Longest Period (CDLP) Without Freshwater Supply at Different Critical Salinity Limit at Chenhang and Qingcaosha Reservoir

		Observation	Modeled critical salinity limit (psu)			
Reservoir	Days without freshwater supply	0.35 psu	0.25	0.5	0.75	1
Chenhang Reservoir	Regular days	68	132	99	**71**	26
	CDLP	–	69	56	28	9
Qingcaosha Reservoir	Regular days	–	166	136	102	64
	CDLP	54	84	67	**54**	37

Note. A (regular) day without freshwater supply is defined as a day without freshwater supply for at least 4 hr. The bold values are the calibrated days compared to the observations.

Table 3
Comparisons Between Averaged Surface Salinity at Qingcaosha Reservoir (km-75) During the Wet Season, Dry Season, and a Full Year, and the Number of (Regular) Days and Consecutive Days of the Longest Period (CDLP) Without Freshwater Supply in a Series of Scenarios (See Table 1)

		Salinity at km-75 (psu)			Without freshwater supply	
Category	Scenarios	Wet	Dry	Year	Regular days	CDLP
With sediment effects	C0-sed	0.009	0.718	0.365	102	54
	C1-sed	0.002	0.356	0.180	14	7
	C2-sed	0.054	1.051	0.554	152	71
	C3-sed	0.036	1.317	0.678	155	71
	C4-sed	0.001	0.397	0.200	24	6
Without sediment effects	C0-hydro	0.001	0.320	0.161	21	5
	C1-hydro	0.001	0.320	0.161	0	0
	C2-hydro	0.011	0.545	0.279	80	13
	C3-hydro	0.012	0.688	0.351	106	26
	C4-hydro	0.001	0.320	0.161	21	5

supply (106), whereas the reduced variability of river discharge (scenario C1-hydro with "HG-Q2" hydrograph) leads to sufficient freshwater throughout the whole year. Therefore, a future decline in sediment loads alleviates other factors potentially threatening freshwater availability (water withdraw, SLR). Moreover, the number of days without freshwater varies between −100% and +405% without full coupling compared to −86% to +52% when accounting for sediments, suggesting that sediments also provide a stabilizing factor on saltwater intrusion.

5. Discussions

Throughout the world, estuaries are impacted by climate change and various human interventions (upstream dam construction, deepening of waterways). Both influence the upestuary boundary conditions (the total river discharge as well as the seasonal variability, the sediment load) and downestuary boundary conditions (tidal dynamics, water depth) which all influence ETM dynamics and saltwater intrusion (Figure 10). A large amount of literature exists relating hydrodynamic changes (river discharge, SLR) to saltwater intrusion (Bhuiyan & Dutta, 2012; Cai et al., 2015; Eslami, Hoekstra, Minderhoud, et al., 2021; Liu & Liu, 2014). At the same time, most river systems experience a decline in sediment loads (Besset et al., 2019; J. Syvitski et al., 2022). However, (future) saltwater intrusion has so far not been related to a reduction in riverine sediment supply. Hereafter, we will briefly evaluate the mechanism through which sediments influence saltwater intrusion, following by a discussion on changing hydrodynamic boundary conditions (through human interventions as well as climate change) and sediment loads.

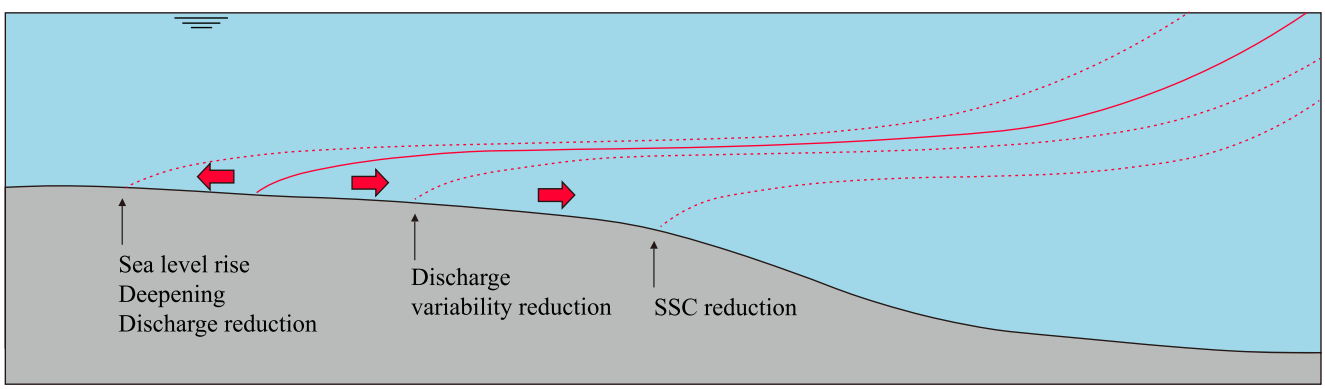

Figure 10. Sea-level rise, deepening, and discharge reduction lead to a landward migration of the saltwater intrusion (red line), whereas a reduction in seasonal variability of river discharge leads to a seaward migration of comparable magnitude (within our scenario space). A 70% reduction in suspended sediment concentration, however, leads to a much more pronounced seaward migration of the saltwater intrusion.

5.1. Sediment Effects on Saltwater Intrusion

The sediment concentration provides feedbacks to hydrodynamics including salinity through a number of complex feedback effects (for details, see C. Zhu, van Maren, et al., 2021; C. Zhu et al., 2022). Classically, an ETM is formed by sediment converging mechanisms resulting from estuarine circulation typically driven by salinity differences and by tidal trapping. An ETM reduces vertical mixing of the water column and therefore promotes saltwater intrusion. The ETM has influences sediment dynamics (and therefore salt dynamics) in the following ways. The longitudinal sediment-induced density gradients lead to divergence of sediment due to the opposite baroclinic pressure gradient upstream and downstream of the maximum SSC of the ETM (i.e., the ETM becomes weaker).

Vertical sediment-induced density gradients, however, may lead to a convergence of sediment in two ways. First, the SSC is higher near the bed than near the surface, introducing a vertical density gradient which reduces vertical mixing and thereby strengthens salinity effects promoting ETM formation. Second, the vertical concentration reduces the effective hydraulic drag due to buoyancy destruction and leads to tidal amplification and deformation, thereby enhancing tidal trapping and thus the ETM formation. At sufficiently high SSC, positive feedback mechanisms therefore exist which lead to progressive trapping of sediments and increasing saltwater intrusion.

Our work therefore reveals that in turbid estuaries (a) sediments need to be accounted for when assessing the impact of hydrodynamic changes, and (b) a change in sediment supply may have a major influence on saltwater intrusion and ETM formation. Both aspects will be elaborated in more detail below.

5.2. River Discharge, Sea-Level Rise, and Channel Deepening

The river discharge has a major impact on the upstream extent of saltwater intrusion. Upstream reservoirs typically lead to a reduction in the higher river discharge and a more even discharge distribution over the year (Biemans et al., 2011). Climate change also influences precipitation (e.g., Dai, 2013) and therefore river discharge. The precipitation is predicted to increase 4.4%–11.1% in most regions of China when global temperature increases by 1.5°C (H. Li et al., 2018). Using a range of climate models, Gao et al. (2020) predict that the average Yangtze discharge and the dry season discharge will decrease during 2070–2099, while changes in the wet season discharge depend on the RCP climate scenarios. Wen et al. (2020), on the other hand, suggest that the mean discharge will increase in the period 2070–2099, whereas the peak discharge will increase and the low discharge will decrease. It is apparently difficult to accurately predict how the Yangtze River discharge will be due to climate change and therefore we have not model climate-change-driven river discharge scenarios. Still, our work does reveal that a reduction of the total river discharge leads to landward intrusion of the salt wedge, whereas a reduced seasonal variation of the river discharge (with a higher minimal river discharge) benefits freshwater supply.

Our work corroborates earlier findings (Bhuiyan & Dutta, 2012; Cai et al., 2015; Liu & Liu, 2014) that SLR leads to stronger saltwater intrusion. Many estuaries which are threatened by SLR are additionally deepened and narrowed, such as the Rhine-Meuse Delta (Vellinga et al., 2014); Tampa Bay (J. Zhu et al., 2014); Elbe Estuary, Ems Estuary, and Loire Estuary (Winterwerp et al., 2013); upper Scheldt Estuary (Z. B. Wang et al., 2019); Columbia Estuary (Jay et al., 2011); and Cape Fear River Estuary (Familkhalili & Talke, 2016), leading to tidal amplification (Ralston & Geyer, 2019; P. Zhang et al., 2021) and stronger saltwater intrusion (Eslami et al., 2019; Lerczak et al., 2009; Monismith et al., 2002). Deepening leads to not only enhanced sediment trapping (Winterwerp & Wang, 2013; Winterwerp et al., 2013) but also stronger estuarine circulation promoting salinity-induced stratification (Chen et al., 2016; Chua & Xu, 2014) and sediment trapping (Burchard & Baumert, 1998; Festa & Hansen, 1978; Geyer & MacCready, 2014), all further strengthening saltwater intrusion (C. Zhu, van Maren, et al., 2021; C. Zhu et al., 2022). Therefore, channel deepening in combination with climate change and SLR is crucial for increasing salinity.

An important finding of our work is also that the predicted impact of hydrodynamic variations (SLR, deepening, and discharge changes) on saltwater intrusion in turbid estuaries is influenced by the effects of sediments. For the Yangtze Estuary, the saltwater intrusion is enhanced by sediment-coupling effects regardless of the hydrodynamic variations. This effect is more pronounced from the bottom isohaline; however, the variation in surface isohaline is vital for freshwater supply under the condition of high estuarine SSC and strong landward extent of the ETM. Moreover, the impact of hydrodynamic variations is larger for a model not accounting for sediments than it is for a fully coupled model (Table 3). SLR, for instance, leads to much more days without fresh water (relative to the reference condition C0) without coupling (85 days or 405%), than with coupling (53 days or 52%).

5.3. Fluvial Sediment Supply

Many major rivers suffer from a decline in sediment supply (Anthony et al., 2015; Besset et al., 2019; Dunn et al., 2019; L. Li, Ni, et al., 2020; J. P. Syvitski et al., 2009) often resulting in coastline erosion. Our results suggest that a decline in sediment load also affects ETM dynamics and saltwater intrusion. The ETM migrates landward as the sediment load decreases, reaching a maximum landward limit at a reduction of 50%–60% after which it propagates seaward again (Figure 7). This partly indicates that for reductions exceeding this limit the effect of the changes in sediment on salinity becomes smaller (although with some exceptions because of the nonlinear response of salinity to changes in sediment; see Figure 8). Note that the ETM location, magnitude as well as its extension determine the effect of sediment on tidal propagation and therefore on the salinity changes. Even though, a lower sediment supply generally alleviates saltwater intrusion and potential future shortages in freshwater availability. In our scenarios, a 70% reduction in sediment load (scenario C4-sed) has an impact on saltwater intrusion which is comparable to the flattening of the river discharge (scenario C1-sed, the most effective hydrodynamic scenario for reducing saltwater intrusion). For scenario C1-sed (C4-sed), the salinity at Qingcaosha Reservoir decreases 0.36 (0.33) psu in the dry season, the days without freshwater availability reduces with 86% (76%), and the surface isohaline migrates 60 km (50 km) seaward (Figure 6 and Table 3). Although the role of hydrodynamic variations (river discharge and SLR) still dominates saltwater intrusion, the effects of reduced sediment supply cannot be neglected, particularly for low discharges and pronounced sediment load reductions.

The positive feedbacks introduced above are, however, only valid for fine-grained sediment (as evaluated in the current work). When the sediment load is primarily composed of sandy sediment, the most prominent impact of a sediment load reduction may be an erosion of the river bed. This effectively deepens the river bed, promoting saltwater intrusion and amplifying the tides. This has been observed, for instance, in the Mekong River (Eslami et al., 2019).

Note that in reality a reduced sediment supply does not immediately result in a reduced sediment concentration in the downstream estuary. Our model suggests that sediment concentration in the estuary decreases from 20 to 1 kg/m^3 with 70% reduced sediment supply. In reality, the response time of an estuary to such an upstream reduction is strongly determined by sediment buffers (on the bed of the tidal channels, but especially on the fringing flats and/or seaward delta front). Such a delayed response is illustrated by the construction of dams such as in the Yangtze. The construction of reservoirs leads to a pronounced reduction of the sediment load immediately downstream of the dam, but this reduction becomes less pronounced in the downstream direction by erosion in the river bed (L. Guo et al., 2021a; X. Guo et al., 2021b; Yuan et al., 2020). Further downstream, the morphological change in the mouth zone of the Yangtze Estuary is suggested to show a time lag of 30 years in response to the reduced sediment supply (C. Zhu et al., 2019). The near-bed sediment concentration in the mouth zone still remains high (>10 kg/m^3) for a long time and only has been decreasing in recent years (C. Zhu, Guo, et al., 2021). Therefore, long-term monitoring the sediment concentration in the estuary in the future is crucial for the uncertainties of the sediment effects.

6. Conclusions

We explored the effect of changes in river discharge, SLR, and sediment supply on saltwater intrusion in the Yangtze Estuary, particularly focusing on the role of sediment dynamics, using a well-calibrated numerical model accounting for effects of sediments on hydrodynamics. A key finding is that a lower fluvial sediment supply reduces saltwater intrusion through its effect on vertical mixing and may thereby potentially positively influence freshwater availability. However, when a sediment reduction also leads to river bed erosion, this reduction may also set in motion processes promoting saltwater intrusion. An intermediate reduction in sediment load leads to the maximum landward of the ETM. In addition, the various river discharge and hydrograph, sediment supply and SLR scenarios lead to an increase in the number of days without freshwater supply by days to months when using a fully coupled model (compared to a noncoupled model without sediment effects). Applying noncoupled models (as commonly done in predicting saltwater intrusion) to estimate the impact of climate change scenarios would therefore erroneously predict the impact of deepening, SLR, or changes in river discharge distribution. However, such an effect could also be minor if estuarine sediment concentration is fairly low and therefore the application of noncoupled model should address the uncertainty of sediments.

Overall, we conclude that although saltwater intrusion is influenced by a large number of potential future scenarios influencing the hydrodynamics (SLR, changes in total discharge, and variability by precipitation changes and reservoirs, as well as local interventions), a previously overlooked aspect that is crucial for turbid estuaries is the role of sediments. Sediments influence saltwater intrusion through complex feedback mechanisms, making future saltwater intrusion even more difficult to predict. Moreover, out of the various scenarios related to climate change and human interventions on saltwater intrusion, the reduction in fluvial sediment supply can also be equally important. In turbid estuaries, studies on (changes in) saltwater intrusion should adequately address the effect of sediment concentration using a fully coupled model.

Data Availability Statement

Data in this study are publicly available at C. Zhu (2023, https://doi.org/10.6084/m9.figshare.14355911).

Acknowledgments
This paper is financially supported by NSFC (U2040216, 42206169, and 51739005), Shanghai Pujiang Program (22PJD020), Shanghai Committee of Science and Technology (20DZ1204700 and 21230750600), and China Postdoctoral Science Foundation (2022M721165). It is also a product of the project "Coping with deltas in transition" within the Programme of Strategic Scientific Alliances between China and the Netherlands (PSA), financed by the Chinese Ministry of Science and Technology (MOST), Project No. 2016YFE0133700, and Royal Netherlands Academy of Arts and Sciences (KNAW), Project No. PSA-SA-E-02. C. Zhu is partially supported by the China Scholarship Council (201506140037).

References

Alfieri, L., Burek, P., Feyen, L., & Forzieri, G. (2015). Global warming increases the frequency of river floods in Europe. *Hydrology and Earth System Sciences*, *19*(5), 2247–2260. https://doi.org/10.5194/hess-19-2247-2015

Anthony, E. J., Brunier, G., Besset, M., Goichot, M., Dussouillez, P., & Nguyen, V. L. (2015). Linking rapid erosion of the Mekong River delta to human activities. *Scientific Reports*, *5*(1), 14745. https://doi.org/10.1038/srep14745

Banas, N., Hickey, B., MacCready, P., & Newton, J. (2004). Dynamics of Willapa Bay, Washington: A highly unsteady, partially mixed estuary. *Journal of Physical Oceanography*, *34*(11), 2413–2427. https://doi.org/10.1175/jpo2637.1

Besset, M., Anthony, E. J., & Bouchette, F. (2019). Multi-decadal variations in delta shorelines and their relationship to river sediment supply: An assessment and review. *Earth-Science Reviews*, *193*, 199–219. https://doi.org/10.1016/j.earscirev.2019.04.018

Bhuiyan, M. J. A. N., & Dutta, D. (2012). Assessing impacts of sea level rise on river salinity in the Gorai River network, Bangladesh. *Estuarine, Coastal and Shelf Science*, *96*, 219–227. https://doi.org/10.1016/j.ecss.2011.11.005

Biemans, H., Haddeland, I., Kabat, P., Ludwig, F., Hutjes, R. W. A., Heinke, J., et al. (2011). Impact of reservoirs on river discharge and irrigation water supply during the 20th century. *Water Resources Research*, *47*(3), W03509. https://doi.org/10.1029/2009WR008929

Brockway, R., Bowers, D., Hoguane, A., Dove, V., & Vassele, V. (2006). A note on salt intrusion in funnel-shaped estuaries: Application to the Incomati Estuary, Mozambique. *Estuarine, Coastal and Shelf Science*, *66*(1–2), 1–5. https://doi.org/10.1016/j.ecss.2005.07.014

Brouwer, R. L., Schramkowski, G. P., Dijkstra, Y. M., & Schuttelaars, H. M. (2018). Time evolution of estuarine turbidity maxima in well-mixed, tidally dominated estuaries: The role of availability- and erosion-limited conditions. *Journal of Physical Oceanography*, *48*(8), 1629–1650. https://doi.org/10.1175/jpo-d-17-0183.1

Burchard, H., & Baumert, H. (1998). The formation of estuarine turbidity maxima due to density effects in the salt wedge. A hydrodynamic process study. *Journal of Physical Oceanography*, *28*(2), 309–321. https://doi.org/10.1175/1520-0485(1998)028<0309:TFOETM>2.0.CO;2

Cai, H., Savenije, H. H., Zuo, S., Jiang, C., & Chua, V. P. (2015). A predictive model for salt intrusion in estuaries applied to the Yangtze Estuary. *Journal of Hydrology*, *529*, 1336–1349. https://doi.org/10.1016/j.jhydrol.2015.08.050

Chen, W., Chen, K., Kuang, C., Zhu, D. Z., He, L., Mao, X., et al. (2016). Influence of sea level rise on saline water intrusion in the Yangtze River Estuary, China. *Applied Ocean Research*, *54*, 12–25. https://doi.org/10.1016/j.apor.2015.11.002

Cheng, X.-j., Zhan, W., Guo, Z.-r., & Yuan, L.-r. (2012). A modeling study on saltwater intrusion to western four watercourses in the Pearl River estuary. *China Ocean Engineering*, *26*(4), 575–590. https://doi.org/10.1007/s13344-012-0044-y

Chua, V. P., & Xu, M. (2014). Impacts of sea-level rise on estuarine circulation: An idealized estuary and San Francisco Bay. *Journal of Marine Systems*, *139*, 58–67. https://doi.org/10.1016/j.jmarsys.2014.05.012

Dai, A. (2013). Increasing drought under global warming in observations and models. *Nature Climate Change*, *3*(1), 52–58. https://doi.org/10.1038/nclimate1633

Dijkstra, Y. M., Schuttelaars, H. M., & Winterwerp, J. C. (2018). The hyperturbid state of the water column in estuaries and rivers: The importance of hindered settling. *Ocean Dynamics*, *68*(3), 377–389. https://doi.org/10.1007/s10236-018-1132-1

Dunn, F. E., Darby, S. E., Nicholls, R. J., Cohen, S., Zarfl, C., & Fekete, B. M. (2019). Projections of declining fluvial sediment delivery to major deltas worldwide in response to climate change and anthropogenic stress. *Environmental Research Letters*, *14*(8), 084034. https://doi.org/10.1088/1748-9326/ab304e

Dyer, K. R. (1997). *Estuaries: A physical introduction* (2nd ed., 195 pp.). John Wiley Sons.

Eslami, S., Hoekstra, P., Kernkamp, H. W. J., Nguyen Trung, N., Do Duc, D., Nguyen Nghia, H., et al. (2021). Dynamics of salt intrusion in the Mekong Delta: Results of field observations and integrated coastal–inland modelling. *Earth Surface Dynamics*, *9*(4), 953–976. https://doi.org/10.5194/esurf-9-953-2021

Eslami, S., Hoekstra, P., Minderhoud, P. S. J., Trung, N. N., Hoch, J. M., Sutanudjaja, E. H., et al. (2021). Projections of salt intrusion in a mega-delta under climatic and anthropogenic stressors. *Communications Earth & Environment*, *2*(1), 142. https://doi.org/10.1038/s43247-021-00208-5

Eslami, S., Hoekstra, P., Nguyen Trung, N., Ahmed Kantoush, S., Van Binh, D., Duc Dung, D., et al. (2019). Tidal amplification and salt intrusion in the Mekong Delta driven by anthropogenic sediment starvation. *Scientific Reports*, *9*(1), 18746. https://doi.org/10.1038/s41598-019-55018-9

Familkhalili, R., & Talke, S. A. (2016). The effect of channel deepening on tides and storm surge: A case study of Wilmington, NC. *Geophysical Research Letters*, *43*, 9138–9147. https://doi.org/10.1002/2016GL069494

Festa, J. F., & Hansen, D. V. (1978). Turbidity maxima in partially mixed estuaries: A two-dimensional numerical model. *Estuarine and Coastal Marine Science*, *7*(4), 347–359. https://doi.org/10.1016/0302-3524(78)90087-7

Gao, C., Su, B., Krysanova, V., Zha, Q., Chen, C., Luo, G., et al. (2020). A 439-year simulated daily discharge dataset (1861–2299) for the upper Yangtze River, China. *Earth System Science Data*, *12*(1), 387–402. https://doi.org/10.5194/essd-12-387-2020

Geyer, W. R., & MacCready, P. (2014). The estuarine circulation. *Annual Review of Fluid Mechanics*, *46*(1), 175–197. https://doi.org/10.1146/annurev-fluid-010313-141302

Gong, W., & Shen, J. (2011). The response of salt intrusion to changes in river discharge and tidal mixing during the dry season in the Modaomen Estuary, China. *Continental Shelf Research*, *31*(7–8), 769–788. https://doi.org/10.1016/j.csr.2011.01.011

Guo, L., Su, N., Zhu, C., & He, Q. (2018). How have the river discharges and sediment loads changed in the Changjiang River basin downstream of the Three Gorges Dam? *Journal of Hydrology*, *560*, 259–274. https://doi.org/10.1016/j.jhydrol.2018.03.035

Guo, L., Zhu, C., Xie, W., Xu, F., Wu, H., Wan, Y., et al. (2021). Changjiang Delta in the Anthropocene: Multi-scale hydro-morphodynamics and management challenges. *Earth-Science Reviews*, *223*, 103850. https://doi.org/10.1016/j.earscirev.2021.103850

Guo, X., Fan, D., Zheng, S., Wang, H., Zhao, B., & Qin, C. (2021). Revisited sediment budget with latest bathymetric data in the highly altered Yangtze (Changjiang) Estuary. *Geomorphology*, *391*, 107873. https://doi.org/10.1016/j.geomorph.2021.107873

Hesse, R. F., Zorndt, A., & Fröhle, P. (2019). Modelling dynamics of the estuarine turbidity maximum and local net deposition. *Ocean Dynamics*, *69*(4), 489–507. https://doi.org/10.1007/s10236-019-01250-w

Hossain, S., Eyre, B. D., & McKee, L. J. (2004). Impacts of dredging on dry season suspended sediment concentration in the Brisbane River estuary, Queensland, Australia. *Estuarine, Coastal and Shelf Science*, *61*(3), 539–545. https://doi.org/10.1016/j.ecss.2004.06.017

Jay, D. A., Leffler, K., & Degens, S. (2011). Long-term evolution of Columbia River tides. *Journal of Waterway, Port, Coastal, and Ocean Engineering*, *137*(4), 182–191. https://doi.org/10.1061/(ASCE)WW.1943-5460.0000082

Jeong, S., Yeon, K., Hur, Y., & Oh, K. (2010). Salinity intrusion characteristics analysis using EFDC model in the downstream of Geum River. *Journal of Environmental Sciences*, *22*(6), 934–939. https://doi.org/10.1016/s1001-0742(09)60201-1

Jeuken, M. C. J. L., & Wang, Z. B. (2010). Impact of dredging and dumping on the stability of ebb–flood channel systems. *Coastal Engineering*, *57*(6), 553–566. https://doi.org/10.1016/j.coastaleng.2009.12.004

Lerczak, J. A., Geyer, W. R., & Ralston, D. K. (2009). The temporal response of the length of a partially stratified estuary to changes in river flow and tidal amplitude. *Journal of Physical Oceanography*, *39*(4), 915–933. https://doi.org/10.1175/2008jpo3933.1

Lesser, G. R., Roelvink, J. A., van Kester, J. A. T. M., & Stelling, G. S. (2004). Development and validation of a three-dimensional morphological model. *Coastal Engineering*, *51*(8–9), 883–915. https://doi.org/10.1016/j.coastaleng.2004.07.014

Li, H., Chen, H., Wang, H., & Yu, E. (2018). Future precipitation changes over China under 1.5°C and 2.0°C global warming targets by using CORDEX regional climate models. *Science of the Total Environment*, *640–641*, 543–554. https://doi.org/10.1016/j.scitotenv.2018.05.324

Li, L., Ni, J., Chang, F., Yue, Y., Frolova, N., Magritsky, D., et al. (2020). Global trends in water and sediment fluxes of the world's large rivers. *Science Bulletin*, *65*(1), 62–69. https://doi.org/10.1016/j.scib.2019.09.012

Li, L., Zhu, J., Chant, R. J., Wang, C., & Pareja-Roman, L. F. (2020). Effect of dikes on saltwater intrusion under various wind conditions in the Changjiang Estuary. *Journal of Geophysical Research: Oceans*, *125*, e2019JC015685. https://doi.org/10.1029/2019JC015685

Li, M., & Chen, Z. (2019). *An assessment of saltwater intrusion in the Changjiang (Yangtze) River Estuary, China, coasts and estuaries* (pp. 31–43). Elsevier.

Liu, W.-C., & Liu, H.-M. (2014). Assessing the impacts of sea level rise on salinity intrusion and transport time scales in a tidal estuary, Taiwan. *Water*, *6*(2), 324–344. https://doi.org/10.3390/w6020324

Monismith, S. G., Kimmerer, W., Burau, J. R., & Stacey, M. T. (2002). Structure and flow-induced variability of the subtidal salinity field in northern San Francisco Bay. *Journal of Physical Oceanography*, *32*(11), 3003–3019. https://doi.org/10.1175/1520-0485(2002)032<3003:SAFIVO>2.0.CO;2

Nguyen, D. H., Umeyama, M., & Shintani, T. (2012). Importance of geometric characteristics for salinity distribution in convergent estuaries. *Journal of Hydrology*, *448–449*, 1–13. https://doi.org/10.1016/j.jhydrol.2011.10.044

Prandle, D. (2004). Saline intrusion in partially mixed estuaries. *Estuarine, Coastal and Shelf Science*, *59*(3), 385–397. https://doi.org/10.1016/j.ecss.2003.10.001

Prandle, D., & Lane, A. (2015). Sensitivity of estuaries to sea level rise: Vulnerability indices. *Estuarine, Coastal and Shelf Science*, *160*, 60–68. https://doi.org/10.1016/j.ecss.2015.04.001

Ralston, D. K., & Geyer, W. R. (2019). Response to channel deepening of the salinity intrusion, estuarine circulation, and stratification in an urbanized estuary. *Journal of Geophysical Research: Oceans*, *124*, 4784–4802. https://doi.org/10.1029/2019JC015006

Ralston, D. K., Geyer, W. R., & Lerczak, J. A. (2008). Subtidal salinity and velocity in the Hudson River Estuary: Observations and modeling. *Journal of Physical Oceanography*, *38*(4), 753–770. https://doi.org/10.1175/2007jpo3808.1

Ralston, D. K., Geyer, W. R., & Lerczak, J. A. (2010). Structure, variability, and salt flux in a strongly forced salt wedge estuary. *Journal of Geophysical Research*, *115*, C06005. https://doi.org/10.1029/2009JC005806

Rice, K. C., Hong, B., & Shen, J. (2012). Assessment of salinity intrusion in the James and Chickahominy Rivers as a result of simulated sea-level rise in Chesapeake Bay, East Coast, USA. *Journal of Environmental Management*, *111*, 61–69. https://doi.org/10.1016/j.jenvman.2012.06.036

Robins, P. E., Skov, M. W., Lewis, M. J., Giménez, L., Davies, A. G., Malham, S. K., et al. (2016). Impact of climate change on UK estuaries: A review of past trends and potential projections. *Estuarine, Coastal and Shelf Science*, *169*, 119–135. https://doi.org/10.1016/j.ecss.2015.12.016

Savenije, H. H. (2006). *Salinity and tides in alluvial estuaries*. Elsevier.

Shi, R., Wang, T., Yang, D., & Yang, Y. (2022). Streamflow decline threatens water security in the upper Yangtze River. *Journal of Hydrology*, *606*, 127448. https://doi.org/10.1016/j.jhydrol.2022.127448

Simpson, J. H., Brown, J., Matthews, J., & Allen, G. (1990). Tidal straining, density currents, and stirring in the control of estuarine stratification. *Estuaries*, *13*(2), 125–132. https://doi.org/10.2307/1351581

Syvitski, J., Ángel, J. R., Saito, Y., Overeem, I., Vörösmarty, C. J., Wang, H., & Olago, D. (2022). Earth's sediment cycle during the Anthropocene. *Nature Reviews Earth & Environment*, *3*(3), 179–196. https://doi.org/10.1038/s43017-021-00253-w

Syvitski, J. P., Kettner, A. J., Overeem, I., Hutton, E. W. H., Hannon, M. T., Brakenridge, G. R., et al. (2009). Sinking deltas due to human activities. *Nature Geoscience*, *2*(10), 681–686. https://doi.org/10.1038/ngeo629

Talke, S. A., de Swart, H. E., & de Jonge, V. N. (2009). An idealized model and systematic process study of oxygen depletion in highly turbid estuaries. *Estuaries and Coasts*, *32*(4), 602–620. https://doi.org/10.1007/s12237-009-9171-y

Talke, S. A., & Jay, D. A. (2020). Changing tides: The role of natural and anthropogenic factors. *Annual Review of Marine Science*, *12*(1), 121–151. https://doi.org/10.1146/annurev-marine-010419-010727

Tang, J., Xu, J., Zhao, S., & Liu, W. (2011). Research on saltwater intrusion of the south branch of the Changjiang Estuary based on measured data (in Chinese). *Resources and Environment in the Yangtze Basin*, *20*(6), 677–684.

Uncles, R., & Stephens, J. (1996). Salt intrusion in the Tweed Estuary. *Estuarine, Coastal and Shelf Science*, *43*(3), 271–293. https://doi.org/10.1006/ecss.1996.0070

van Maanen, B., & Sottolichio, A. (2018). Hydro- and sediment dynamics in the Gironde estuary (France): Sensitivity to seasonal variations in river inflow and sea level rise. *Continental Shelf Research*, *165*, 37–50. https://doi.org/10.1016/j.csr.2018.06.001

van Maren, D. S., van Kessel, T., Cronin, K., & Sittoni, L. (2015). The impact of channel deepening and dredging on estuarine sediment concentration. *Continental Shelf Research*, *95*, 1–14. https://doi.org/10.1016/j.csr.2014.12.010

van Maren, D. S., Vroom, J., Fettweis, M., & Vanlede, J. (2020). Formation of the Zeebrugge coastal turbidity maximum: The role of uncertainty in near-bed exchange processes. *Marine Geology*, *425*, 106186. https://doi.org/10.1016/j.margeo.2020.106186

van Maren, D. S., Winterwerp, J. C., Decrop, B., Wang, Z. B., & Vanlede, J. (2011). Predicting the effect of a current deflecting wall on harbour siltation. *Continental Shelf Research*, *31*(10), S182–S198. https://doi.org/10.1016/j.csr.2010.12.005

van Maren, D. S., Winterwerp, J. C., & Vroom, J. (2015). Fine sediment transport into the hyper-turbid lower Ems River: The role of channel deepening and sediment-induced drag reduction. *Ocean Dynamics*, *65*(4), 589–605. https://doi.org/10.1007/s10236-015-0821-2

Vellinga, N., Hoitink, A., van der Vegt, M., Zhang, W., & Hoekstra, P. (2014). Human impacts on tides overwhelm the effect of sea level rise on extreme water levels in the Rhine–Meuse delta. *Coastal Engineering*, *90*, 40–50. https://doi.org/10.1016/j.coastaleng.2014.04.005

Wan, Y., & Zhao, D. (2017). Observation of saltwater intrusion and ETM dynamics in a stably stratified estuary: The Yangtze Estuary, China. *Environmental Monitoring and Assessment*, *189*(2), 89. https://doi.org/10.1007/s10661-017-5797-6

Wang, J., Li, L., He, Z., Kalhoro, N. A., & Xu, D. (2019). Numerical modelling study of seawater intrusion in Indus River Estuary, Pakistan. *Ocean Engineering*, *184*, 74–84. https://doi.org/10.1016/j.oceaneng.2019.05.029

Wang, Z. B., Vandenbruwaene, W., Taal, M., & Winterwerp, H. (2019). Amplification and deformation of tidal wave in the upper Scheldt estuary. *Ocean Dynamics*, *69*(7), 829–839. https://doi.org/10.1007/s10236-019-01281-3

Watanabe, K., Kasai, A., Antonio, E. S., Suzuki, K., Ueno, M., & Yamashita, Y. (2014). Influence of salt-wedge intrusion on ecological processes at lower trophic levels in the Yura Estuary, Japan. *Estuarine, Coastal and Shelf Science*, *139*, 67–77. https://doi.org/10.1016/j.ecss.2013.12.018

Wen, S., Su, B., Wang, Y., Zhai, J., Sun, H., Chen, Z., et al. (2020). Comprehensive evaluation of hydrological models for climate change impact assessment in the Upper Yangtze River Basin, China. *Climatic Change*, *163*(3), 1207–1226. https://doi.org/10.1007/s10584-020-02929-6

Winterwerp, J. C., & Wang, Z. B. (2013). Man-induced regime shifts in small estuaries—I: Theory. *Ocean Dynamics*, *63*(11–12), 1279–1292. https://doi.org/10.1007/s10236-013-0662-9

Winterwerp, J. C., Wang, Z. B., van Braeckel, A., van Holland, G., & Kösters, F. (2013). Man-induced regime shifts in small estuaries—II: A comparison of rivers. *Ocean Dynamics*, *63*(11–12), 1293–1306. https://doi.org/10.1007/s10236-013-0663-8

Wolanski, E., Ngoc Huan, N., Trong Dao, L., Huu Nhan, N., & Ngoc Thuy, N. (1996). Fine-sediment dynamics in the Mekong River Estuary, Vietnam. *Estuarine, Coastal and Shelf Science*, *43*(5), 565–582. https://doi.org/10.1006/ecss.1996.0088

Wu, H., Zhu, J., & Ho Choi, B. (2010). Links between saltwater intrusion and subtidal circulation in the Changjiang Estuary: A model-guided study. *Continental Shelf Research*, *30*(17), 1891–1905. https://doi.org/10.1016/j.csr.2010.09.001

Wu, S., Cheng, H., Xu, Y. J., Li, J., & Zheng, S. (2016). Decadal changes in bathymetry of the Yangtze River Estuary: Human impacts and potential saltwater intrusion. *Estuarine, Coastal and Shelf Science*, *182*, 158–169. https://doi.org/10.1016/j.ecss.2016.10.002

Xue, P., Chen, C., Ding, P., Beardsley, R. C., Lin, H., Ge, J., & Kong, Y. (2009). Saltwater intrusion into the Changjiang River: A model-guided mechanism study. *Journal of Geophysical Research*, *114*, C02006. https://doi.org/10.1029/2008JC004831

Yang, S. L., Milliman, J., Xu, K., Deng, B., Zhang, X., & Luo, X. (2014). Downstream sedimentary and geomorphic impacts of the Three Gorges Dam on the Yangtze River. *Earth-Science Reviews*, *138*, 469–486. https://doi.org/10.1016/j.earscirev.2014.07.006

Yuan, B., Lin, B., & Sun, J. (2020). Decadal changes in sediment budget and morphology in the tidal reach of the Yangtze River. *Catena*, *188*, 104438. https://doi.org/10.1016/j.catena.2019.104438

Zhang, E., Gao, S., Savenije, H. H., Si, C., & Cao, S. (2019). Saline water intrusion in relation to strong winds during winter cold outbreaks: North Branch of the Yangtze Estuary. *Journal of Hydrology*, *574*, 1099–1109. https://doi.org/10.1016/j.jhydrol.2019.04.096

Zhang, E., Savenije, H. H., Wu, H., Kong, Y., & Zhu, J. (2011). Analytical solution for salt intrusion in the Yangtze Estuary, China. *Estuarine, Coastal and Shelf Science*, *91*(4), 492–501. https://doi.org/10.1016/j.ecss.2010.11.008

Zhang, P., Yang, Q., Wang, H., Cai, H., Liu, F., Zhao, T., & Jia, L. (2021). Stepwise alterations in tidal hydrodynamics in a highly human-modified estuary: The roles of channel deepening and narrowing. *Journal of Hydrology*, *597*, 126153. https://doi.org/10.1016/j.jhydrol.2021.126153

Zhu, C. (2023). Impact of reduced fluvial sediment supply on saltwater intrusion in the Yangtze Estuary [Dataset]. figshare. https://doi.org/10.6084/m9.figshare.14355911

Zhu, C., Guo, L., van Maren, D. S., Tian, B., Wang, X., He, Q., & Wang, Z. B. (2019). Decadal morphological evolution of the mouth zone of the Yangtze Estuary in response to human interventions. *Earth Surface Processes and Landforms*, *44*(12), 2319–2332. https://doi.org/10.1002/esp.4647

Zhu, C., Guo, L., van Maren, D. S., Wang, Z. B., & He, Q. (2021). Exploration of decadal tidal evolution in response to morphological and sedimentary changes in the Yangtze Estuary. *Journal of Geophysical Research: Oceans*, *126*, e2020JC017019. https://doi.org/10.1029/2020JC017019

Zhu, C., van Maren, D. S., Guo, L., Lin, J., He, Q., & Wang, Z. B. (2021). Effects of sediment-induced density gradients on the estuarine turbidity maximum in the Yangtze Estuary. *Journal of Geophysical Research: Oceans*, *126*, e2020JC016927. https://doi.org/10.1029/2020JC016927

Zhu, C., van Maren, D. S., Guo, L., Lin, J., He, Q., & Wang, Z. B. (2022). Feedback effects of sediment suspensions on transport mechanisms in an estuarine turbidity maximum. *Journal of Geophysical Research: Oceans*, *127*, e2021JC018029. https://doi.org/10.1029/2021JC018029

Zhu, J., Gu, Y., & Wu, H. (2013). Determination of the period not suitable for taking domestic water supply to the Qingcaosha Reservoir near Changjiang River Estuary (in Chinese). *Oceanologia et Limnologia Sinica/Hai Yang Yu Hu Chao*, *44*(5), 1138–1145.

Zhu, J., Weisberg, R. H., Zheng, L., & Han, S. (2014). Influences of channel deepening and widening on the tidal and nontidal circulations of Tampa Bay. *Estuaries and Coasts*, *38*(1), 132–150. https://doi.org/10.1007/s12237-014-9815-4

Zhu, J., Wu, H., Li, L., & Qiu, C. (2018). *Saltwater intrusion in the Changjiang Estuary, coastal environment, disaster, and infrastructure—A case study of China's coastline*. IntechOpen.

References From the Supporting Information

Allen, J., Somerfield, P., & Gilbert, F. (2007). Quantifying uncertainty in high-resolution coupled hydrodynamic-ecosystem models. *Journal of Marine Systems*, *64*(1–4), 3–14. https://doi.org/10.1016/j.jmarsys.2006.02.010

Chu, A., Wang, Z., De Vriend, H., & Stive, M. (2010). A process-based approach to sediment transport in the Yangtze Estuary. Paper presented at 32nd International Conference on Coastal Engineering, ICCE 2010, Shanghai, China.

Egbert, G. D., Bennett, A. F., & Foreman, M. G. (1994). TOPEX/POSEIDON tides estimated using a global inverse model. *Journal of Geophysical Research*, *99*(C12), 24821–24852. https://doi.org/10.1029/94JC01894

Egbert, G. D., & Erofeeva, S. Y. (2002). Efficient inverse modeling of barotropic ocean tides. *Journal of Atmospheric and Oceanic Technology*, *19*(2), 183–204. https://doi.org/10.1175/1520-0426(2002)019<0183:EIMOBO>2.0.CO;2

Hu, K. L., Ding, P. X., Zhu, S. X., & Cao, Z. Y. (2000). 2-D current field numerical simulation integrating Yangtze Estuary with Hangzhou Bay. *China Ocean Engineering*, *14*(1), 89–102.

Partheniades, E. (1965). Erosion and deposition of cohesive soils. *Journal of the Hydraulics Division*, *91*(1), 105–139. https://doi.org/10.1061/jyceaj.0001165

Pawlowicz, R., Beardsley, B., & Lentz, S. (2002). Classical tidal harmonic analysis including error estimates in MATLAB using T_TIDE. *Computers & Geosciences*, *28*(8), 929–937. https://doi.org/10.1016/s0098-3004(02)00013-4

Richardson, J. F., & Zaki, W. N. (1954). Sedimentation and fluidization: Part I. *Transactions of the Institution of Chemical Engineers*, *32*, 35–53.

Wan, Y., & Wang, L. (2017). Numerical investigation of the factors influencing the vertical profiles of current, salinity, and SSC within a turbidity maximum zone. *International Journal of Sediment Research*, *32*(1), 20–33. https://doi.org/10.1016/j.ijsrc.2016.07.003

Winterwerp, J. (2007). On the deposition flux of cohesive sediment. *Proceedings in Marine Science*, *8*, 209–226.

Yun, C. (2004). *Recent development of the Changjiang Estuary* (320 pp., in Chinese with abstract in English). China Ocean Press.

Zhu, L., He, Q., Shen, J., & Wang, Y. (2016). The influence of human activities on morphodynamics and alteration of sediment source and sink in the Changjiang Estuary. *Geomorphology*, *273*, 52–62. https://doi.org/10.1016/j.geomorph.2016.07.025